Dynamics of a three-mass system with cubic nonlinearity and that of an equivalent electrical circuit

Vladimirs Nikishins[1], Ivans Grinevichs[2], Igors Scukins[3]
RTU Daugavpils Study and Science Centre, Riga Technical University, Daugavpils, Latvia
[1]Corresponding author
E-mail: [1]*vladimirs.nikisins@rtu.lv*, [2]*ivans.grinevics@rtu.lv*, [3]*igors.scukins@rtu.lv*

Received 30 March 2022; received in revised form 2 August 2022; accepted 10 August 2022
DOI https://doi.org/10.21595/jve.2022.22539

Abstract. The paper considers the reaction of a mechanical system of three masses connected by springs and absorbers moving in the longitudinal direction to the action of a harmonic force applied to the largest mass. This mass is attached to the base by a spring with cubic nonlinearity, while smaller masses are connected to the main mass by linear springs. A method is proposed for obtaining the amplitude-frequency characteristic (AFC) of a nonlinear system from the AFC sequence of linearized systems. The results of modelling an equivalent electrical circuit, which is an analogue of a mechanical system, are presented. The influence of the value of the nonlinearity coefficient on the dynamic response of systems has been studied. It is noted that for some combinations of values of the system parameters with cubic nonlinearity with mass ratios m_1:m_2:m_3 = 4:2:1, the AFC contains outer and inner isolated areas – islands.

Keywords: the three-mass nonlinear system, equivalent electric circuit, dynamic response, linearization.

1. Introduction

Models of two or three masses connected by nonlinear springs and absorbers are often used to describe various mechanisms: vibration isolation systems such as a suspension of a vehicle, an industrial robot cutting arm, a punching press, an impact tool, a gyroscope, a generator. The vehicle suspension is modelled in [1-5] by a system of three masses with springs and absorbers. The system parameters that ensure the driver's comfort and safety are determined using a wavelet analysis. In [6-9] a system with two degrees of freedom consists of a large-mass linear oscillator and a low-mass nonlinear vibration absorber. Free and forced oscillations of the system are studied using the theory of normal modes and perturbation methods. In [7], the dynamics of a linear oscillator is studied for a similar model by the averaging method. The goal is to reduce the amplitude of the oscillator near resonance by adjusting the parameters of the nonlinear absorber. It is shown that both a positive influence of a nonlinear absorber and a negative one in the appearance of unstable modes leading to dangerous instability, are possible. Various complex motions associated with these instabilities are studied by the method of direct numerical integration.

The universal software package SPRING, designed to study various problems of the dynamics of nonlinear systems, was used in to study the bifurcations of single-mass systems with different types of nonlinearities.

The vibration microgyroscope in [10] consists of three masses, two masses oscillate in the longitudinal direction, and the third one can also oscillate in the transverse direction, absorbing the vibrations of the active mass. This design, in combination with the proposed technological methods, improves the quality of the gyroscope. In [11], a model of a vibro-impact triboelectric generator with three degrees of freedom is presented. The impact of various ratios of masses and distances between them on the dynamic response and the generated energy has been studied. It is concluded that symmetric mass configurations of the oscillator are energetically more favourable than asymmetric cases.

The aim of paper [12] is to analyse the discrete dynamic behaviour of nonlinear intelligent mechanical vibration systems with co-located sensors and actuating units. To illustrate the theory, a numerical example of a system with two masses is given. The considered approach is proposed to be applied to systems with three masses.

2. Equations of motion

The mechanical system (MS) is described (Fig. 1) by the system of equations:

$$\begin{cases} m_1\ddot{x}_1 + (b_1 + b_2)\dot{x}_1 - b_2\dot{x}_2 + (k_1 + k_2)x_1 + kx_1^3 - k_2x_2 = F_m \sin(\omega t), \\ m_2\ddot{x}_2 - b_2\dot{x}_1 + (b_2 + b_3)\dot{x}_2 - b_3\dot{x}_3 - k_2x_1 + (k_2 + k_3)x_2 - k_3x_3 = 0, \\ m_3\ddot{x}_3 - b_3\dot{x}_2 + b_3\dot{x}_3 - k_3x_2 + k_3x_3 = 0, \end{cases} \quad (1)$$

where m_1, m_2, m_3– masses of bodies; b_1, b_2, b_3 – damping coefficient; k_1, k_2, k_3 – linear coefficients of spring stiffness; k – nonlinear coefficient of the 1st spring ($k_1x + kx^3$ – cubic nonlinearity); F_m – amplitude of the harmonic force applied to the 1st mass.

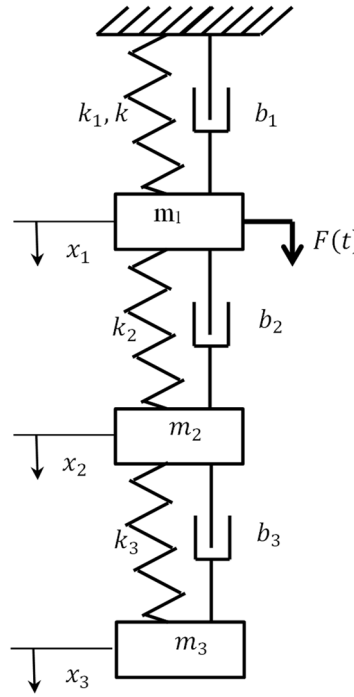

Fig. 1. Mechanical system with three masses

The electrical circuit (EC) is described (Fig. 2) by a system of equations compiled according to the method of loop currents:

$$\begin{cases} L_1\dfrac{dj_1}{dt} + R_1j_1 + \dfrac{1}{C_1}\int j_1dt + R_2(j_1 - j_2) + \dfrac{1}{C_2}\int (j_1 - j_2)dt = e(t), \\ L_2\dfrac{dj_2}{dt} - R_2(j_1 - j_2) - \dfrac{1}{C_2}\int (j_1 - j_2)dt + R_3(j_2 - j_3) + \dfrac{1}{C_3}\int (j_2 - j_3)dt = 0, \\ L_3\dfrac{dj_3}{dt} + R_3(j_3 - j_2) + \dfrac{1}{C_3}\int (j_3 - j_2)dt = 0, \end{cases} \quad (2)$$

where L_k – inductance ($k = 1, 2, 3$); R_k – resistors resistance; C_k – capacitor capacity; j_k – loop currents. Given that the amount of electricity from the loop current $Q_k = \int j_k dt$, the system of equations of the loop current method (2) can be written in the following form:

$$\begin{cases} L_1\ddot{Q}_1 + (R_1 + R_2)\dot{Q}_1 - R_2\dot{Q}_2 + (S_1 + S_2)Q_1 + SQ_1^3 - S_2Q_2 = E_m \sin(\omega t), \\ L_2\ddot{Q}_2 - R_2\dot{Q}_1 + (R_2 + R_3)\dot{Q}_2 - R_3\dot{Q}_3 - S_2Q_1 + (S_2 + S_3)Q_2 - S_3Q_3 = 0, \\ L_3\ddot{Q}_3 - R_3\dot{Q}_2 + R_3\dot{Q}_3 - S_3Q_2 + S_3Q_3 = 0, \end{cases} \quad (3)$$

where $S_k = 1/C_k$ – inverse capacitance, $S = 0$ for the linear system, E_m – amplitude of harmonic voltage of the generator.

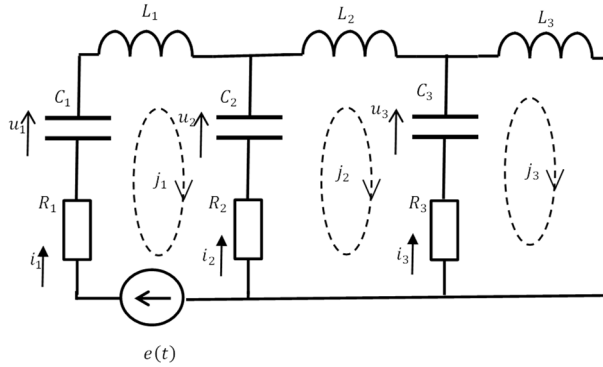

Fig. 2. Equivalent electrical circuit

Capacitor currents are expressed in terms of loop currents:

$$\begin{cases} i_1 = j_1, \\ i_2 = j_2 - j_1, \\ i_3 = j_3 - j_2, \end{cases} \quad (4)$$

and the charges (amounts of electricity) of the capacitors are equal to $q_k = \int i_k dt$, then the ratios for the quantities of electricity of capacitors and the quantities of electricity from loop currents are true:

$$\begin{cases} q_1 = Q_1, \\ q_2 = Q_2 - Q_1, \\ q_3 = Q_3 - Q_2, \end{cases} \quad (5)$$

and the voltages of the capacitors are found by the formulas $u_1 = S_1 q_1 + S(q_1)^3$, $u_k = S_k q_k$ ($k = 2, 3$). To reduce the equations of motion of a mechanical system to dimensionless parameters, the following expressions are used:

$$m_0 = m_3, \quad x_0 = \frac{F_m}{k_3}, \quad t_0 = 2\pi\sqrt{\frac{m_0}{k_3}}, \quad \tilde{m}_k = \frac{m_k}{m_0}, \quad \tilde{x}_k = \frac{x_k}{x_0}, \quad \tilde{t} = \frac{t}{t_0}, \quad \tilde{\omega} = \omega t_0,$$

$$\tilde{b}_k = b_k\frac{t_0}{m_0}, \quad \tilde{k}_k = k_k\frac{t_0^2}{m_0}, \quad \tilde{k} = k\frac{x_0^2 \cdot t_0^2}{m_0}, \quad \tilde{F}_m = F_m\frac{t_0^2}{m_0 x_0}, \quad (k = 1,2,3),$$

where the sign "~" denotes dimensionless parameters. After substituting these expressions and transformations into the system of differential equations of motion of a mechanical system, a system of equations in dimensionless parameters will be obtained. The form of the resulting

system of equations, after discarding the "~" sign from the symbols, coincides with the form of the dimensional system. The above equations of motion of a mechanical system are also true for dimensionless parameters.

To reduce the equations of motion of the electrical system to dimensionless parameters, the following expressions are used:

$$L_0 = L_3, \quad Q_0 = \frac{E_m}{S_3}, \quad t_0 = 2\pi\sqrt{\frac{L_0}{S_3}}, \quad \tilde{L}_k = \frac{L_k}{L_0}, \quad \tilde{Q}_k = \frac{Q_k}{Q_0}, \quad \tilde{t} = \frac{t}{t_0}, \quad \tilde{\omega} = \omega t_0 ,$$
$$\tilde{R}_k = R_k \frac{t_0}{L_0}, \quad \tilde{S}_k = S_k \frac{t_0^2}{L_0}, \quad \tilde{S} = S \frac{Q_0^2 \cdot t_0^2}{L_0}, \quad \tilde{E}_m = E_m \frac{t_0^2}{L_0 Q_0},$$
$$\tilde{u}_k = \frac{u_k t_0^2}{L_0 Q_0}, \quad (k = 1,2,3) ,$$

where the sign "~" denotes dimensionless parameters. Performing operations similarly to the case of a mechanical system leads to a dimensionless system of differential equations of an electrical circuit. The form of the resulting system of equations, after discarding the sign "~" from the symbols, coincides with the form of the dimensional system. The above equations of the electrical system are also true for dimensionless parameters.

Comparison of the equations for MS and EC leads to a well-known analogy between them (Table 1).

Table 1. Analogy between the parameters of mechanical and electrical systems

Mass m_k, kg	Inductance L_k, H
Damping coefficient b_k, N·s/m	Resistance R_k, Ω
Elastic coefficient k_k, N/m	Inverse capacitance S_k, F^{-1}
Mass displacement x_k, m	The amount of electricity of the loop current Q_k, C
Velocity $\dot{x}_k$, m/s	Loop current j_k, A
Force of spring elasticity, N	Capacitor voltage u_k, V
Force F_k, N	Electromotive force E_m, V

Taking into account this analogy, the method is described below only for a mechanical system.

Normal form of equations for the mechanical system (Fig. 1):

$$\begin{cases} \dot{x}_1 = x_4, \\ \dot{x}_2 = x_5, \\ \dot{x}_3 = x_6, \\ \dot{x}_4 = \dfrac{1}{m_1}[F_m \sin \omega t + k_2 x_2 - (k_1 + k_2)x_1 - k x_1^3 + b_2 x_5 - (b_1 + b_2)x_4], \\ \dot{x}_5 = \dfrac{1}{m_2}[k_3 x_3 - (k_2 + k_3)x_2 + k_2 x_1 + b_3 x_6 - (b_2 + b_3)x_5 + b_2 x_4], \\ \dot{x}_6 = \dfrac{1}{m_3}[k_3 x_2 - k_3 x_3 - b_3 x_6 + b_3 x_5], \end{cases} \tag{6}$$

where $x_{1,2,3}$ – displacements of the 1st, 2nd, 3rd masses; $x_{4,5,6}$ – velocity of the 1st, 2nd, 3rd masses; circular frequency $1 < \omega < 13$; time $0 < t < 70$. Parameter values: $m_1 = 4$; $m_2 = 2$; $m_3 = 1$ – masses of bodies; $b_1 = 1$; $b_2 = 0.3$; $b_3 = 0.3$ – damping coefficients; $k_1 = 100$; $k_2 = 25$; $k_3 = 40$ – linear coefficients of spring forces; $k = 20 \ldots 400$ nonlinear coefficient of the 1st spring ($k_1 x + k x^3$ – cubic nonlinearity); $F_m = 40$ – the amplitude of the force applied to the 1st mass. The numerical solution (NS) for a normal system was obtained by the Runge-Kutta method in the SPRING program [13], developed to study dynamic processes in nonlinear systems.

3. Analytical solution method

"Energy" linearization (EL) is the replacement of nonlinear equations with linear ones based on the equality of potential energies of equally deformed nonlinear and equivalent linear springs. Let the force and deformation of a nonlinear spring be related by the relation:

$$F_n = k_1 x + k x^3, \tag{7}$$

and for an equivalent linear spring, this relationship has the form:

$$F_e = k_e x, \tag{8}$$

where $k_e - const$, for a specific deformation x. From the equality of potential energies of equally deformed springs:

$$\int_0^x F_e dx = \int_0^x F_n dx, \quad \int_0^x k_e x dx = \int_0^x k_1 x + k x^3 dx, \tag{9}$$

the equivalent coefficient of elasticity of a linear spring is found:

$$k_e(x) = k_1 + \frac{1}{2} k x^2. \tag{10}$$

With "force" linearization (FL), the forces of equally deformed nonlinear and equivalent linear springs are equated:

$$F_n = F_e, \tag{11}$$

and the equivalent coefficient of elasticity of the linear spring is found:

$$k_e(x) = k_1 + k x^2. \tag{12}$$

In the general case, the equivalent coefficient of elasticity of a linear spring for a cubic nonlinearity can be written as:

$$k_e(x) = k_1 + s k x^2, \tag{13}$$

where s – weight coefficient, $0.5 \le s \le 1$. The minimum value of the weight coefficient $s = 0.5$ corresponds to EL, and the maximum value $s = 1$ corresponds to FL.

Formally, when solving the system of MS equations, we can put $k = 0$ and $k_1 = k_e(x_1)$. The resulting linear system is solved by the method of complex amplitudes, as a result of which the system of differential equations is reduced to a system of linear algebraic equations for complex amplitudes:

$$A \cdot \begin{pmatrix} \dot{X}_1 \\ \dot{X}_2 \\ \dot{X}_3 \end{pmatrix} = \begin{pmatrix} F_m \\ 0 \\ 0 \end{pmatrix}, \tag{14}$$

where $\dot{X}_n = X_n \cdot e^{j \cdot \varphi_n}$ – complex displacement amplitude x_n ($n = 1, 2, 3$); hereinafter, the dot above the symbol denotes the complex nature of the value , and not differentiation with respect to time, as it was in the systems of equations, $j = \sqrt{-1}$ – imaginary unit; $x_n = \mathrm{Im}\left(\dot{X}_n e^{j \cdot \omega t}\right) = X_n \sin(\omega t + \varphi_n)$; A – matrix of coefficients with elements $a_{11} = -m_1 \omega^2 + j\omega(b_1 + b_2) + k_e +$

$k_e + k_2$, $a_{12} = -k_2 - j\omega b_2$, $a_{13} = 0$, $a_{21} = -k_2 - j\omega b_2$, $a_{22} = -m_2\omega^2 + j\omega(b_2 + b_3) + k_2 + k_3$, $a_{23} = -k_3 - j\omega b_3$, $a_{31} = 0$, $a_{32} = -k_3 - j\omega b_3$, $a_{33} = k_3 + j\omega b_3 - m_3\omega^2$.

According to Cramer's formulae, the solution to the system of linear algebraic equations of complex amplitudes has the form:

$$\dot{X}_n = \frac{\Delta_n}{\det A(\omega, k_e)}, \quad (n = 1,2,3), \tag{15}$$

where the numerator and denominator are complex polynomials with respect to frequency ω. For example:

$$\Delta_n = A_n(F_m, \omega) + jB_n(F_m, \omega), \tag{16}$$

where

$$A_1(F_m, \omega) = F_m(m_2m_3\omega^4 - (b_2b_3 + k_2m_3 + k_3m_2 + k_3m_3)\omega^2 + k_2k_3),$$
$$B_1(F_m, \omega) = F_m(-(b_2m_3 + b_3m_2 + b_3m_3)\omega^3 + (b_2k_3 + b_3k_2)\omega),$$
$$A_2(F_m, \omega) = F_m(-(b_2b_3 + k_2m_3)\omega^2 + k_2k_3),$$
$$B_2(F_m, \omega) = F_m(-(b_2m_3)\omega^3 + (b_2k_3 + b_3k_2)\omega),$$
$$A_3(F_m, \omega) = F_m(-(b_2b_3)\omega^2 + k_2k_3),$$
$$B_3(F_m, \omega) = F_m(b_2k_3 + b_3k_2)\omega.$$

Moduli of complex amplitudes:

$$X_n = \frac{|\Delta_n|}{|\det A(\omega, k_e)|}, \quad (n = 1,2,3), \tag{17}$$

after squaring:

$$X_n^2 = \frac{|\Delta_n|^2}{|\det A(\omega, k_e)|^2}, \tag{18}$$

will be the ratio of real polynomials with respect to frequency ω. Expression for $\det A(\omega, k_e)$ with Eq. (12) for FL:

$$k_e = k_1 + k \cdot X_1^2, \tag{19}$$

will be as follows:

$$detA(\omega, X_1) = U(\omega) + jW(\omega) + Z(\omega)X_1^2 + jT(\omega)X_1^2, \tag{20}$$

where:

$$T(\omega) = k\left(\omega(b_2k_3 + b_3k_2) + \omega^3\left((-b_3 - b_2)m_3 - b_3m_2\right)\right),$$
$$Z(\omega) = k\left(k_2k_3 - \omega^2\left((k_3 + k_2)m_3 + (k_3m_2 + b_2b_3)\right) + \omega^4m_2m_3\right). \tag{21}$$

The polynomials $U(\omega)$ and $W(\omega)$ can be written as the scalar product of vectors:

$$U(\omega) = (U_1 \quad U_2 \quad U_3 \quad U_4)\begin{pmatrix} 1 \\ \omega^2 \\ \omega^4 \\ \omega^6 \end{pmatrix}, \tag{22}$$

where the coordinates of the first term are the coefficients of a polynomial with even powers of the cyclic frequency:

$$\begin{aligned} U_1 &= k_1k_2k_3, \\ U_2 &= \Big(\big((k_2+k_1)k_3+k_1k_2\big)m_3+(k_2+k_1)k_3m_2+k_2k_3m_1+b_1b_2k_3+b_1b_3k_2 \\ &\quad +b_2b_3k_1\Big), \\ U_3 &= \big((k_2+k_1)m_2+(k_3+k_2)m_1+(b_2+b_1)b_3+b_1b_2\big)m_3 \\ &\quad +(k_3m_1+(b_2+b_1)b_3)m_2+b_2b_3m_1, \\ U_4 &= -m_1\cdot m_2\cdot m_3\,. \end{aligned} \tag{23}$$

Similarly:

$$W(\omega)=(W_1 \quad W_2 \quad W_3)\begin{pmatrix}\omega\\ \omega^3\\ \omega^5\end{pmatrix}, \tag{24}$$

here the coordinates of the first vector are the coefficients of a polynomial with odd powers of cyclic frequency:

$$\begin{aligned} W_1 &= (b_1k_2+b_2k_1)k_3+b_3k_1k_2, \\ W_2 &= \Big(\big((b_2+b_3)k_3+(b_3+b_1)k_2+(b_3+b_2)k_1\big)m_3 \\ &\quad +\big((b_2+b_1)k_3+b_3k_2+b_3k_1\big)m_2+(b_2k_3+b_3k_2)m_1+b_1b_2b_3\Big), \\ W_3 &= \big((b_2+b_1)m_2+(b_3+b_2)m_1\big)m_3+b_3m_1m_2. \end{aligned} \tag{25}$$

Substituting Eq. (20) for $\det A(\omega, X_1)$ into for Eq. (18) of the squared amplitude for $n=1$, after transformations, we obtain the expression:

$$X_1^2=\frac{A_1^2(F_m,\omega)+B_1^2(F_m,\omega)}{\big(Z(\omega)\cdot X_1^2+U(\omega)\big)^2+\big(T(\omega)\cdot X_1^2+W(\omega)\big)^2}, \tag{26}$$

which is a cubic equation with respect to the square of the modulus $(X_1)^2$:

$$\begin{aligned} &(Z(\omega)^2+T(\omega)^2)\cdot X_1^6+2\big(U(\omega)Z(\omega)+W(\omega)T(\omega)\big)\cdot X_1^4+(U(\omega)^2+W(\omega)^2)\cdot X_1^2 \\ &\quad -A_1(F_m,\omega)^2-B_1(F_m,\omega)^2=0. \end{aligned} \tag{27}$$

By setting ω, roots X_1 are found from this equation and the amplitude-frequency characteristic (AFC) is constructed for the first approximation of the nonlinear system. With one real root of the cubic equation, MS has one stable mode, and with three real roots, two stable and one unstable modes. The ambiguity X_1 is taken into account when determining the displacement amplitudes of other masses X_2 and X_3. The described method was implemented in the Mathcad software.

4. Graphic analogue of the method

The method presented above is an analytical implementation of a graphical method for determining AFC of the nonlinear MS from AFC of the linear MS. Graphically, the AFC of the nonlinear MS can be found from the AFC of the linear MS using the following algorithm:

1. Set the initial value of displacement x_1;

2. Determine the coefficient of equivalent stiffness of the nonlinear MC for the given displacement $k_e(x_1)$ according to the chosen linearization method (EL, FL);

3. Assume the parameter k_1 of a linear MS to be equal to the coefficient of equivalent stiffness

$k_1 = k_e(x_1)$;

4. Construct the AFC of the linear MS of point 3;

5. Draw a horizontal line L at level x_1 on the AFC of point 4;

6. Determine the coordinates of the points of intersection of line L with the AFC. If there are no intersection points, then exit the algorithm;

7. The points in 6 belong to the AFC of the nonlinear MS and are marked on its graph;

8. The displacement value x_1 is increased by the amount of the selected step. Go to point 2.

If you need to find the AFC of the nonlinear EC, then the graphical method has specific features and is as follows:

1. Set the initial value of the amount of electricity Q_1 (analogue of displacement x_1);

2. Determine the equivalent inverse capacitance $S_e(Q_1) = S_1 + S(Q_1)^2$ (FL);

3. Parameter S_1 is assumed to be equal to the equivalent inverse capacitance $S_1 = S_e(Q_1)$;

4. Find capacitance $C_1 = 1/S_1$;

5. Determine dimensional parameter (real capacitance) C_{r1};

6. Determine voltage $u_1 = S_1 Q_1$ across capacitor C_1;

7. Determine the dimensional parameter (the real voltage across capacitor C_{r1}) $u_{r1} = u_1(L_0 Q_0)/t_0^2$;

8. Construct the AFC of the linear EC with capacitor C_{r1};

9. Draw a horizontal line L on the AFC of point 8 at level u_{r1};

10. Determine the coordinates of the points of intersection of line L with the AFC. If there are no intersection points, then exit the algorithm;

11. The points in 10 belong to the AFC of the nonlinear EC and are marked on its graph;

12. The value of the amount of electricity Q_1 is increased by the value of the selected step. Go to point 2.

An example is given below for the EC graphical algorithm. Let the dimensionless parameters of the MS be known: $m_1 = 4$; $m_2 = 2$; $m_3 = 1$; $b_1 = 1$; $b_2 = 0.3$; $b_3 = 0.3$; $k_1 = 100$; $k_2 = 25$; $k_3 = 40$; $k = 60$; $F_m = 40$.

Using the analogy between MS and EC, the dimensionless parameters of the EC are found: $L_1 = 4$; $L_2 = 2$; $L_3 = 1$; $R_1 = 1$; $R_2 = 0.3$; $R_3 = 0.3$; $S_1 = 100$; $S_2 = 25$; $S_3 = 40$; $S = 60$; $E_m = 40$. To obtain the dimensional parameters of EC, three parameters must be set in an arbitrary way, let them be $L_3 = 0.1$ H, $C_3 = 470$ pF, $E_m = 1$ V, then, using the relationship between the dimensional and dimensionless parameters, the remaining dimensional parameters of the EC are found (4 digits are retained): $L_1 = 0.4$ H; $L_2 = 0.2$ H; $R_1 = 2322$ Ω; $R_2 = 696$ Ω; $R_3 = 696$ Ω; $C_1 = 185.5$ pF; $C_2 = 742.2$ pF. The electrical circuit of the dimensional EC is designed in the Multisim program (Fig. 3). The AFC of the linear EC are obtained using the Bode Plotter tool (Fig. 4). By moving the marker along the AFC, the coordinates of the desired points of the curve are determined.

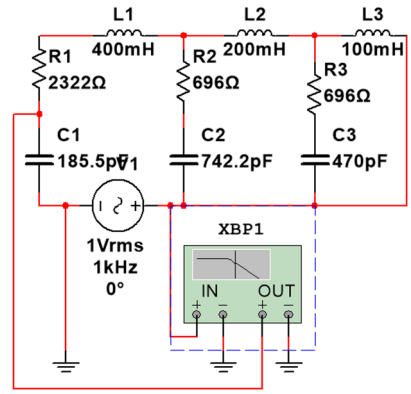

Fig. 3. Dimensional EC in the Multisim program

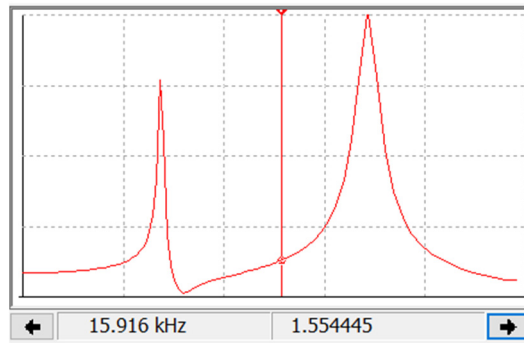

Fig. 4. AFC of the dimensional EC in the Bode Plotter tool window of the Multisim program with a movable vertical marker (in the lower part of the window on the left is the frequency and on the right is the corresponding ordinate of the marker's intersection point with the graph)

Fig. 5 shows the AFC of the dimensional EC recalculated to the dimensional parameters for FL and the simulation results (graphical algorithm), which the centres of the circles correspond to.

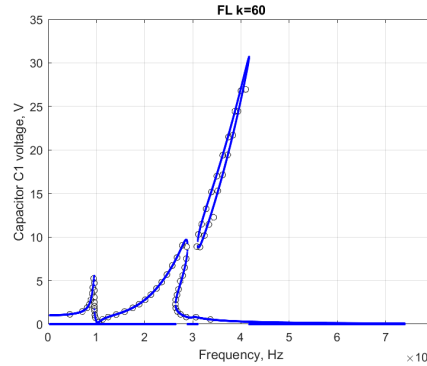

Fig. 5. The recalculated AFC of the dimensional EC and the results of the graphical algorithm (centres of circles) obtained in program multisim

5. Results

The results of the influence of a change in the coefficient of nonlinearity κ on the shape of the AFC of a three-mass system are presented in the graphs Fig. 6, 7, 8.

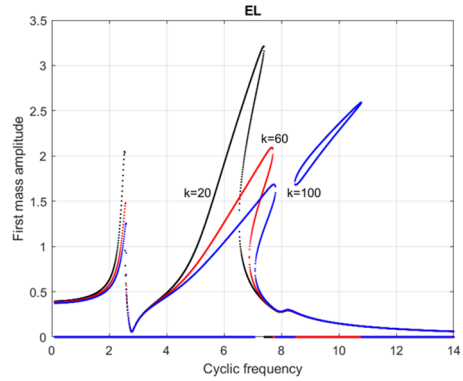

Fig. 6. AFC of the dimensionless MS at EL for nonlinearity coefficients $k = 20, 60$ without singularities and at $k = 100$ with a detached part of the vertex – the "outer island"

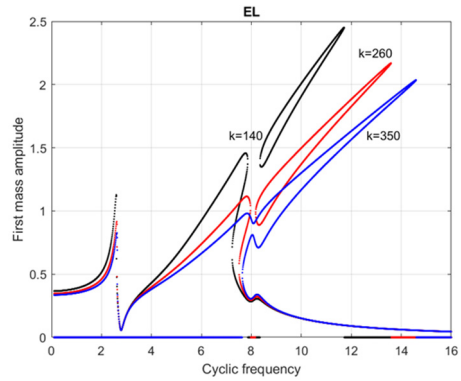

Fig. 7. AFC of dimensionless MS at EL for coefficients of nonlinearity $k = 140, 260$, there is an increase in the size of the "outer island" and at $k = 350$ the "outer island" joins the vertex with the beginning of the formation of the "inner island" under it

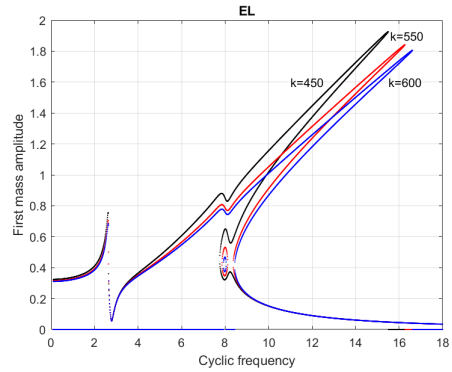

Fig. 8. AFC of dimensionless MS at EL for coefficients of nonlinearity $k = 450$ continuation of the formation of the "inner island", $k = 550$ completion of its formation and $k = 600$ reduction of its size

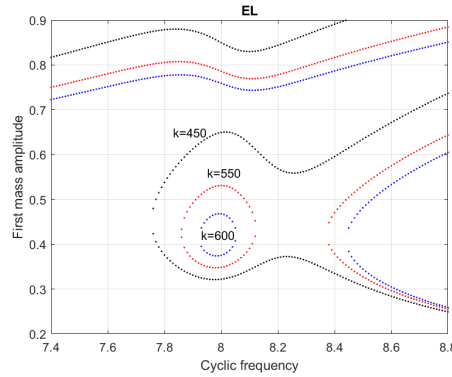

Fig. 9. The enlarged part of the graphs in Fig. 8 showing the emergence of an "inner island" and reducing its size (with a further increase in k, the island shrinks to a point and disappears)

Graphs for the same nonlinearity coefficients for the EL and FL and their comparison with the NS is demonstrated in Fig. 10, 11.

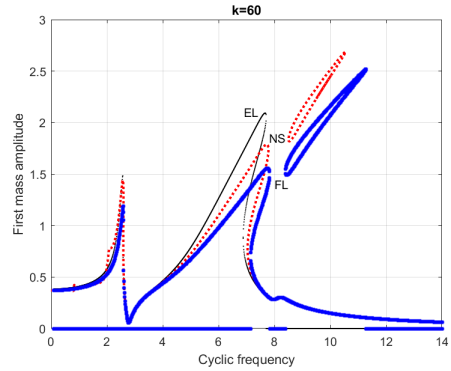

Fig. 10. Comparison of the AFC of the dimensionless MC at EL (there is no "outer island") and FL (the "outer island" increases and approaches the vertex) with NS (increase in the size of the "outer island" that has arisen) for a coefficient of nonlinearity $k = 60$ (NS is the numerical integration of the system (6) in SPRING program)

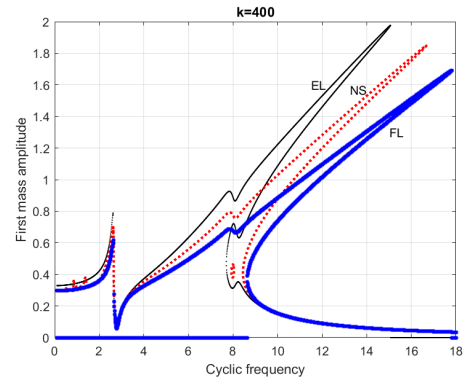

Fig. 11. Comparison of the AFC of the dimensionless MS at EL (the beginning of the formation of the "inner island") and FL (the "inner island" has disappeared) with NS (there is an "inner island") for a nonlinearity coefficient $k = 400$

At close to zero values of the nonlinearity coefficient κ the AFC of the dimensionless MS has three partial resonances: at $\omega_1 = 2.3$ and $\omega_2 = 6$ clearly expressed and at $\omega_3 = 8.2$ hardly noticeable, what can be seen on the graph Fig. 6. for $k = 20$ (the slope of the vertex of the second resonance is due to non-linearity). An increase in the nonlinearity coefficient causes a transformation of the AFC, which can be conditionally divided into the following stages:

1) the appearance of an "outer island" of small size (a point). By "outer island" here we mean a separate area of the AFC graph that is not related to the main AFC, having no features. For example, the main AFC in Fig. 6 there will be curves for $k = 20$ $k = 60$, and the graph for $k = 100$ consists of the main curve and the "outer island". The difference between the "outer island" and the "inner island" is that if you draw a vertical straight line through a separate area of the graph and move along this straight line from the abscissa axis upwards, then for the "outer island" the first point of intersection of the vertical will be with the main AFC, and the second and the third intersection point will be with the boundaries of the "outer island". For the "inner island", the first and second points of intersection of the vertical line, when moving up along, will be with the boundaries of the "inner island", and the third point of intersection will be with the main AFC.

2) Increasing the size of the "outer island", as seen in Fig. 7 for graphs at $k = 140$ and $k = 260$.

3) Contact and merging of the "outer island" with the main AFC, which is illustrated by the graph in Fig. 7 at $k = 350$.

4) Formation of the "inner island" under the spot of merging (their point 3). This process can be traced in the graphs in Fig. 7 at $k = 350$ and 8 for $k = 450$, the merging occurs at the dimensionless cyclic frequency $\omega = 8$.

5) The emergence of the "inner island", for example, in Fig. 8 at $k = 550$ and the zoomed image in Fig. 9 at $k = 550$.

6) The reduction in the size of the "inner island" can be seen in Fig. 8 for $k = 600$ and zoomed in Fig. 9 for $k = 600$.

7) The disappearance of the "inner island", after which the AFC remains, an example of it is given in Fig. 11 for FL.

The curves in Fig.10, 11 show that the MS considered at EL (weight coefficient $s = 0.5$) is less rigid, and at FL ($s = 1$) it is more rigid than the true MS, for which the NS takes place, which is taken here as a benchmark. Any value of the weight coefficient from the interval (0.5;1), for example $s = 0.75$, will give a smaller deviation of the linearized solution from the benchmark.

6. Conclusions

The paper proposes a method for constructing the AFC of a nonlinear system from the set of the AFC of the corresponding linearized systems. It is shown that the benchmark response of a nonlinear system obtained in the SPRING program is the interval between the responses of systems linearized in force and energy. By choosing the optimal weight coefficient, one can achieve the minimum deviation of the approximate solution from the benchmark. Algorithms for graphical construction of the AFC of a nonlinear mechanical system and an equivalent electrical circuit are presented, which graphically implement the proposed analytical method. The influence of the value of the nonlinearity coefficient on the dynamic response of systems has been studied. It has been shown that for some values of the parameters of systems with cubic nonlinearity, the AFC contains outer and inner isolated areas – islands, and the process of the appearance and disappearance of such islands has been illustrated.

Acknowledgements

The authors have not disclosed any funding.

Data availability

The datasets generated during and/or analyzed during the current study are available from the corresponding author on reasonable request.

Conflict of interest

The authors declare that they have no conflict of interest.

References

[1] K. Nouri, H. Loussifi, and N. B. Braiek, "Modelling and wavelet-based identification of 3-DOF vehicle suspension system," *Journal of Software Engineering and Applications*, Vol. 4, No. 12, pp. 672–681, 2011, https://doi.org/10.4236/jsea.2011.412079

[2] Zaripov, R., Gavrilovs, and P., "Assessment of the economic efficiency of modernization of railway wagons," in *Transport Means 2020*, pp. 906–909, 2020.

[3] Gavrilovs, P., Dmitrijevs, and A., "Research in passenger car bogie central suspension roller and rod base metal and welded metal structure," in *Engineering for Rural Development*, pp. 618–623, 2016.

[4] R. T. U. Zaripov and P. Gavrilovs, "Mechanical connection of metal structures in wagon buildings," in *Engineering for Rural Development. Proceedings of the International Scientific Conference (Latvia)*, pp. 596–604, 2021.

[5] Gavrilovs, P., Gorbachovs, and D., "Hardness testing and chemical composition analysis of ER2 and ER2T series emus traction transmission rubber-cord coupling bolts," in *Engineering for Rural Development*, pp. 326–330, 2020.

[6] Y. V. Mikhlin and S. N. Reshetnikova, "Dynamical interaction of an elastic system and essentially nonlinear absorber," *Journal of Sound and Vibration*, Vol. 283, No. 1-2, pp. 91–120, May 2005, https://doi.org/10.1016/j.jsv.2004.03.061

[7] S. Natsiavas, "Dynamics of multiple-degree-of-freedom oscillators with colliding components," *Journal of Sound and Vibration*, Vol. 165, No. 3, pp. 439–453, Aug. 1993, https://doi.org/10.1006/jsvi.1993.1269

[8] Sergejevs, D., Tipainis, A., Gavrilovs, and P., "The restoration of worn surfaces of railway turnout elements by a flux cored arc welding (FCAW)," in *Transport Means 2014*, pp. 24–26, 2014.

[9] Iščuka et al., "Improvement of technology of operation for Daugavpils marshalling station by building the new receiving yard," in *Transport Means 2019*, pp. 841–846, 2019.

[10] R. I. Shakoor, S. A. Bazaz, M. Kraft, Y. Lai, and M. M. Ul Hassan, "Thermal actuation based 3-dof non-resonant microgyroscope using MetalMUMPs," *Sensors*, Vol. 9, No. 4, pp. 2389–2414, Apr. 2009, https://doi.org/10.3390/s90402389

[11] Y. Fu, H. Ouyang, and R. B. Davis, "Nonlinear dynamics and triboelectric energy harvesting from a three-degree-of-freedom vibro-impact oscillator," *Nonlinear Dynamics*, Vol. 92, No. 4, pp. 1985–2004, Jun. 2018, https://doi.org/10.1007/s11071-018-4176-3

[12] I. Andreeva and A. Andreev, "Investigation of a family of cubic dynamic systems," *Vibroengineering Procedia*, Vol. 15, pp. 88–93, Dec. 2017, https://doi.org/10.21595/vp.2017.19389

[13] I. T. Schukin, M. V. Zakrzhevsky, Y. M. Ivanov, V. V. Kugelevich, V. E. Malgin, and Y. V. Frolov, "Application of software SPRING and method of complete bifurcation groups for the bifurcation analysis of the nonlinear dynamical system," *Journal of Vibroengineering*, Vol. 10, No. 4, pp. 510–518, 2008.

Vladimirs Nikishins received his Ph.D. in Engineering from the Moscow Institute of Irrigation and Reclamation at the Department of Structural Mechanics in 1987 in Moscow, Russian Federation. Now he works at Riga Technical University in Daugavpils. The main direction of the research work is the problems of mechanics associated with the dynamics of nonlinear mechanical systems.

Ivans Grinevichs received Dr.sc.ing. degree in the Riga Technical University, Riga, Latvia, in 2012. Now he works at Riga Technical University in Daugavpils. His current research interests include fixed screw joints and assembly automation..

Igors Schukins received Dr.sc.ing. degree in the Riga Technical University, Riga, Latvia, in 2005. Now he works at Riga Technical University in Daugavpils. His current research interests include chaos and bifurcation analysis of dynamical systems.